Science of the Total Environment 748 (2020) 141137

Contents lists available at ScienceDirect

Science of the Total Environment

journal homepage: www.elsevier.com/locate/scitotenv

# A proxy-based approach to predict spatially resolved emissions of macro- and microplastic to the environment

Delphine Kawecki, Bernd Nowack *

*Empa — Swiss Federal Laboratories for Materials Science and Technology, Technology and Society Laboratory, Lerchenfeldstrasse 5, CH-9014 St. Gallen, Switzerland*

## HIGHLIGHTS

- Macro- and microplastic emissions were regionalized for 7 different polymers
- Geographical datasets on land-use statistics were used as proxies
- Emissions to freshwaters and different types of soils were considered
- High resolution (100 × 100 m) emission maps were obtained for Switzerland

## GRAPHICAL ABSTRACT

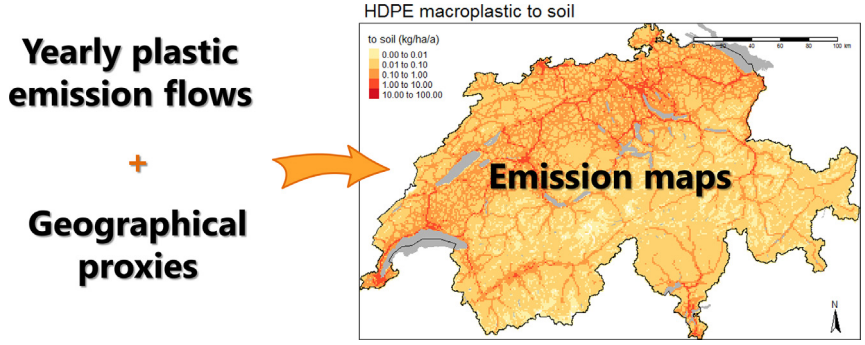


## ARTICLE INFO

*Article history:*
Received 15 June 2020
Received in revised form 16 July 2020
Accepted 19 July 2020
Available online 21 July 2020

Editor: Damia Barcelo

*Keywords:*
Plastic
Microplastics
Emissions
Modelling
Spatial

## ABSTRACT

Large disparities on micro- and macroplastic concentrations are to be expected between residential, industrial, natural and agricultural areas, since specific uses of plastic will determine the magnitude of the corresponding emissions. The aim of this work was to develop a method to regionalize emissions of macroplastic and microplastic for soil, freshwater and air using geographical datasets on land-use statistics, traffic and population densities, wastewater treatment plants and combined sewer overflows as proxies. High resolution maps of the emissions were then generated for micro- and macroplastic using emission data available for Switzerland for seven commonly used polymers (low-density-polyethylene, high-density-polyethylene (HDPE), polypropylene (PP), polystyrene, expanded polystyrene, polyvinyl-chloride and polyethylene-terephthalate). Most of the emissions can be found in areas with high human activity, but the influence of the different proxies varies for each polymer. The median emission rate of macroplastic on soil varies from 0.0006 to 0.06 kg/ha/year, whereas no emission flows are predicted for more than 50% of the raster cells for microplastic regardless of the polymer, but the maxima can reach up to 12.7 kg/ha/a in the case of HDPE. The average emission rate of macroplastic along river segments ranges between 0.062 kg/km/a and 1.5 kg/km/a. For microplastic, the average emission rate varies from 0.0025 kg/km/a to 0.11 kg/km/a. The analysis reveals that a significant deviation is expected if the population density is used as only proxy. The correlation between the population density and the predicted emissions is only $r = 0.16–0.23$ for a cell size of 100 × 100 m and goes up to $r = 0.86–0.88$ for a resolution of 10 km, however an r of only 0.56–0.68 is observed for those polymers used a lot in agriculture such as HDPE and PP. The emission maps obtained in this work can serve as input to regionalized fate models for macro- and microplastics.



* Corresponding author.
*E-mail address:* nowack@empa.ch (B. Nowack).

https://doi.org/10.1016/j.scitotenv.2020.141137

## 1. Introduction

Plastic can be found in nearly every environmental sample in marine and continental environments and is present either as small particles called microplastic (MP) or as larger debris often referred to as macroplastic (Hartmann et al., 2019). Most of the MP research has focussed on the marine environment but research in freshwater environments has intensified (Eerkes-Medrano et al., 2015) and MP has been reported in a wide range of concentrations all over the world (Koelmans et al., 2019; Rios Mendoza and Balcer, 2018). First estimates of MP pollution in soils suggested that it may be considerable as well (de Souza Machado et al., 2017; Nizzetto et al., 2016) but this compartment was up to now much less studied than freshwaters (Eerkes-Medrano et al., 2015; Horton et al., 2017). Macroplastic litter is intimately connected to the MP issue since macroplastic may eventually fragment into MP under environmental conditions but is in comparison to MP much less studied in terrestrial contexts (Bauer-Civiello et al., 2019; Castro-Jiménez et al., 2019; Gasperi et al., 2014; Kiessling et al., 2019; Morritt et al., 2014; Rech et al., 2014). Macroplastic pollution in soils has, to our knowledge, only been examined in the context of citizen science studies focussing on littering (Schultz et al., 2013) or roadsides (Cascadia Consulting Group Inc., 2005).

The sources and pathways of plastic to the environment are increasingly known (Essel et al., 2015; Kawecki and Nowack, 2019; Ryberg et al., 2019) although large uncertainties remain. The largest sources are mismanaged macroplastic and rubber wear particles (Essel et al., 2015; Sieber et al., 2019) (if rubber particles are to be considered MP (Hartmann et al., 2019)), but they are strongly dependent on the polymer considered (Kawecki and Nowack, 2019). Most of the macroplastic emissions originate from mismanagement of waste through littering, dumping and other types of improper disposal of consumer goods and, in a European context, waste from construction sites and agriculture (Kawecki and Nowack, 2019).

The concentration of MP in freshwater has been suggested to depend on the location (Eerkes-Medrano et al., 2015) but as well on the time of sampling since weather (Browne et al., 2010; Dris et al., 2015; Fischer et al., 2016; Goldstein et al., 2013) and currents have been shown to influence it (Eriksen et al., 2013; Mani et al., 2016). On the other hand, the concentration of MP in small streams was shown to be of the same order of magnitude as for large rivers (Dikareva and Simon, 2019), suggesting that the input into small streams may be more relevant than previously expected. Conflicting results on the influence of the population density and combined sewer overflows (CSOs) on MP concentrations were reported (Dikareva and Simon, 2019; Wagner et al., 2019). The spatial variation and dynamics of MP in freshwater is therefore yet to be understood fully. Macroplastic debris in freshwater may be correlated to the population density (Battulga et al., 2019) but few studies have yet investigated the relationship between the burdens in soil and freshwaters. MP contents in soil may be strongly location-dependent because the different emission routes may dominate individual locations (Scheurer and Bigalke, 2018; Zubris and Richards, 2005).

Plastic transport may be very different depending on the density of the material (Hoellein et al., 2019; Schwarz et al., 2019) and the emissions are strongly affected by the life-cycle of the product (Kawecki and Nowack, 2019). It is not yet clear if a difference in toxicity can be expected for the different polymers themselves (Adam et al., 2019; Zimmermann et al., 2019) but it is reasonable to assume variations in additive toxicity depending on the material considered. A polymer-specific assessment of their possible fate and risk is therefore necessary.

Spatially resolved models have recently emerged as a solution for understanding the distribution and variation of pollutants across ecosystems (Lebreton et al., 2017; Unice et al., 2019). These tools typically contain two distinct parts: a first model describing the input into environmental systems and a second model for the fate processes in the environment. The emission flows of commodity plastics to the environment in Switzerland have been published recently (Kawecki and Nowack, 2019), considering Switzerland as a whole region and neglecting any local variations. The next step towards predicted environmental concentrations requires a regionalization of these emission flows.

The aim of the present study was to develop a method to quantify the spatially resolved releases of MP and macroplastic to water, soil and air based on a regional polymer-specific release model. The model was then applied to predict the spatially resolved releases of seven different polymers to the Swiss environment.

## 2. Method

### 2.1. Emission flows

The emission flows of seven polymers into the environment in Switzerland were estimated in an earlier study (Kawecki and Nowack, 2019) using probabilistic material flow analysis. The polymers considered were low-density and high-density polyethylene (LDPE and HDPE, respectively), polypropylene (PP), polystyrene (PS), expanded PS (EPS), polyvinyl chloride (PVC) and polyethylene terephthalate (PET) which are the plastic materials most commonly reported in freshwater environments (Koelmans et al., 2019). A total of 134 processes model the life-cycle and the emission flows, interconnected with a total of 402 flows of which 234 are for modelling emission. The life-cycle comprised the phases production and manufacturing, consumption, waste collection, recycling and waste treatment. Emissions of MP (particles smaller than 5 mm) and macroplastic (plastic pieces larger than 5 mm) were modelled separately, either directly reaching the final environmental compartment or flowing through intermediate compartments such as for example wastewater treatment plants (WWTP), littering and sweeping, organic waste collection and indoor air. The 61 flows connected to surface water, soil and air were considered within this study –releases to subsurface soil were excluded. The emission flows are available as probability distributions (Kawecki and Nowack, 2019) (Fig. S1), of which only the mean and the 5th and 95th percentiles will be considered in the current work.

### 2.2. Proxies

In a first step, each emission flow needs to be transformed into an emission map. To do so, the available geographical datasets (geodataset) of existing statistics were reviewed, and the best fitting geodataset per emission flow was selected and used as proxy for the spatial distribution of the emission flow. The criteria used for choosing a proxy were: a) best correspondence between the emission flow's estimated spatial distribution and the geodataset, and b) geodataset availability. The location of emissions can be surmised from the emission flow itself, since some information is already included in the emission model (Kawecki and Nowack, 2019). The distinction between natural soil, residential soil, agricultural soil and road side soil already made for the emission flow calculations facilitates this process. The reasoning for the best correspondence between the emission flow and the geodataset for each proxy is explained in more detail in the following paragraphs. In total, eleven different geographical proxies were used to regionalize the 61 emission flows (Table S1). For soil and air emissions, six raster maps were created using official statistics. For emissions to water, five more proxies were created. All raster maps were available with a 100 m resolution. The vector maps had a precision of 1:25000.

Before describing each proxy in more detail, a few examples of emission flow and their attributed proxies will be mentioned (for a complete overview, see Table 1). Emissions caused by private consumers occur where these private consumers are at the moment of emission. For any consumer behaviour resulting in an emission outdoors in residential areas, we identified the population density as the closest available match. For any emission resulting from consumer behaviour in natural

environments we used a map of natural areas. Last, for any emission resulting from consumer behaviour in traffic, we used a map of the traffic density. All emissions pertaining to agriculture were regionalized using the geographical distribution of agricultural activities over Switzerland. For emissions originating from industry, the location of industry within Switzerland was used.

### 2.3. Population density

A map of the population density was used for all nine emissions occurring in residential areas (Table S1) as for example the emission of litter to residential soil or the emissions of fibres from clothing or building textiles to outdoor air or soil, respectively, during the use-phase. For this, the total permanent residing population in 2014 was obtained from an online available geographical dataset (geodataset) collected by the Swiss Federal Statistical Office (FSO) (Swiss Federal Statistical Office, 2013, 2017, 2018). The geocoding of the residing population in this geodataset was primarily performed using the localization of buildings intended for habitation and the federal registry for buildings and habitations. The present study uses the freely available geodataset in which, for privacy protection purposes, values below 3 inhabitants/ha are replaced by 3 inhabitants/ha by the FSO.

### 2.4. Land use statistics

Land use statistics from the FSO were used to create proxy maps for industrial, agricultural and natural areas. The original geodataset was created based on aerial photographs verified with other available datasets and point verifications (Swiss Federal Statistical Office, 2013). The available land use statistics were divided into 17 classes for the geodataset developed for 2004–2009.

Two classes were considered for the creation of the industry proxy: industrial and artisanal areas (corresponding to class 1) and special infrastructure areas (4). This proxy was used for the 19 emissions caused by the manufacturing of plastic goods, and the collection and recycling of end-of-life plastic (Table S1).

Similarly, two classes were considered for the creation of the agriculture proxy: fruit arboriculture, viticulture and horticulture (6), and arable land (7). The agriculture proxy was used for all 12 emission flows related to agricultural activities as for example losses of MP from agricultural films and pipes to agricultural soil, or the application of compost containing plastic to land (Table S1).

The last proxy developed based on land use statistics aimed at describing all areas which are of natural character. Six different classes were considered for this proxy: natural prairies and pastureland (8), forest (10), shrubland (11), other woods (12), unproductive vegetation (15) and surfaces without vegetation (16). The proxy for forests and other natural areas was used for the three emission flows occurring on rural soil as for example littering or the release of shotgun cartridges to soil (Table S1).

### 2.5. New buildings

A map of the areas with newly constructed buildings was used for the four emission flows from construction and demolition sites as for example the release of MP from construction pipes to soil or MP from insulation to outdoor air (Table S1). The statistic on buildings and habitations was used for this, from which the number of new buildings for habitation built between 2006 and 2010 were considered (Swiss Federal Statistical Office, 2017). The geocoding of the buildings in the original geodataset was based on the federal registry for buildings and habitations and completed with additional information when necessary.

### 2.6. Traffic

The traffic density in Switzerland was used to regionalize the emissions from littering during transport and from the accidental release of plastic from vehicles (Table S1). The traffic density was obtained from sonBASE, a model developed to predict noise levels induced by traffic in Switzerland (Senozon AG im Auftrag des Bundesamts für Umwelt BAFU, 2017). The model is based on the road network from Openstreetmap, combined with an agent-based model and hourly measurements of traffic density at 1954 locations. The modelled average number of vehicles per day per road segment was used to create the geodataset. All road segments corresponding to tunnels were previously removed.

### 2.7. Area surrounding water bodies

The properties of the areas surrounding water bodies needed to be characterized in a geodataset to be able to distinguish emissions to water occurring around residential or natural areas. Emissions to water in natural environments can occur from littering or shotgun cartridges (Table S1). Emissions to water in residential environments only occur from littering. Both these emission flows were calculated as emissions to water in the original publication (Kawecki and Nowack, 2019) and do not reflect the transport of plastic items from soil to water, but only direct emissions to water through human activities as previously modelled.

Geographical information on the water bodies in Switzerland was obtained from a database from the Swiss Federal Office for the Environment (FOEN) containing the river network, drainage basins and lakes at a precision of 1:25000 (Federal Office for the Environment FOEN, 2015). The geodataset contains 20,167 river segments and 210 polygons for the lakes. The average river segment length is 1.6 km but can vary from 11 m to 18 km. Polygons representing the portions of lakes outside of Switzerland are available in the dataset and will be displayed as grey polygons in the results section, except for the Italian part of Lago Maggiore, which is not present in the initial dataset. The first proxy was calculated by counting the number of inhabitants in a radius of 500 m around each water body. The second proxy was built by counting the number of cells corresponding to forests and other natural environments in a radius of 500 m around the water body. The calculation of the number of cells or inhabitants surrounding a water body was performed in R using the *extract* function from the R package *raster* and using a buffer of 500 m.

### 2.8. Wastewater treatment plants and sewer overflows

Emissions occurring from wastewater treatment plants (WWTPs) were regionalized using WWTP locations and the number of inhabitants connected. The level of treatment of the WWTPs enabled to differentiate between emissions from secondary and tertiary treatment. The WWTP geodataset was combined from two separate datasets available from the FOEN. Starting from the first dataset (Federal Office for the Environment FOEN, 2017), the WWTP identification number, location or address, and the number of inhabitants connected to the WWTP could be obtained for 759 WWTPs. Two out of 759 WWTPs in the dataset did not have any information regarding the number of inhabitants connected and were excluded from the dataset. For 73 of these WWTPs, no coordinates were present in the dataset. The available postal address was then automatically translated into coordinates using OSM Nominatim (OpenStreetMap Foundation, 2019) in an R script. The treatment type of the WWTP was obtained from a second dataset (Federal Office for the Environment FOEN, 2011). Out of all the 759 WWTPs in the primary dataset, 37 are absent from the treatment dataset and 212 are unknown but present in the treatment dataset. For all of these WWTPs, we assume that the highest treatment stage corresponds to secondary treatment.

**Table 1**
Complete overview of the emission flows included and description of the proxies. The colour is representative of the receiving environmental compartment and size of plastic emitted (dark colour: macroplastic, pale colour: microplastic).

| Type of emission flow | Full list of emission flows | Location of the emission | Closest proxy available |
|---|---|---|---|
| Emissions originating from agriculture (including application of compost and digestate onto agricultural soil) | Agricultural pack. films to Agricultural soil<br>Agricultural pack. bottles to Agricultural soil<br>Agricultural films to Agricultural soil<br>Agricultural pipes to Agricultural soil<br>Agricultural other to Agricultural soil<br>Agrotextiles to Agricultural soil<br>Compost to Agricultural soil | Agricultural soil, can also depend on the crop type | Land use statistics: areas used for agriculture |
| | Agricultural films to Agricultural soil (MP)<br>Agricultural pipes to Agricultural soil (MP)<br>Agricultural other to Agricultural soil (MP)<br>Agrotextiles to Agricultural soil (MP)<br>Compost (MP) to Agricultural soil (MP) | | |
| Emissions originating from building and construction | Construction pipes to Residential soil (MP) | Around the construction sites | Statistic on newly built buildings |
| | Insulation (construction) to Outdoor air (MP) | | |
| Emissions originating from the plastic production or manufacturing industry | Second. mat. production to Residential soil (MP)<br>Transport to Residential soil (MP)<br>Fibre production to Residential soil (MP)<br>Non-text. manufacturing to Residential soil (MP) | Around the facilities | Land use statistics: areas used for industry |
| Emissions originating from waste management | Packaging collection to Residential soil<br>Mixed waste collection to Residential soil<br>Agri. waste collection to Residential soil<br>Text. waste collection to Residential soil | Around the facilities | Land use statistics: areas used for industry |
| | Pre-cons. plastic collection to Residential soil (MP)<br>Pre-cons. fibre collection to Residential soil (MP)<br>Packaging recycling to Residential soil (MP)<br>C&D recycling to Residential soil (MP)<br>Auto. large parts recycling to Residential soil (MP)<br>ASR recycling to Residential soil (MP)<br>WEEP recycling to Residential soil (MP)<br>Agri. plastic recycling to Residential soil (MP) | | |
| | ASR recycling to Outdoor air (MP)<br>WEEP recycling to Outdoor air (MP) | | |
| Emissions from miscellaneous industry | Industry water (MP) to Residential soil (MP) | Around the facilities | Land use statistics: areas used for industry |
| Emissions originating from consumer activities | Clothing to Outdoor air (MP)<br>Household textiles to Outdoor air (MP)<br>Technical clothing to Outdoor air (MP)<br>Technical household text. to Outdoor air (MP)<br>Indoor air (MP) to Outdoor air (MP) | Location depends on the activities of the consumer | Population density |
| | Litter (residential) to Residential soil | | |
| | Litter (residential) to Surface water | | Population density around the water bodies |
| Emissions in residential areas not linked to consumer activities | Compost to Residential soil<br>Building textiles to Residential soil<br>Geotextiles to Residential soil | Residential areas | Population density |
| | Compost (MP) to Residential soil (MP)<br>Fabric coatings to Residential soil (MP) | | |
| Emissions along road sides | Automotive to Road side<br>Litter (roads) to Road side | Road sides | Traffic density |

**Table 1** *(continued)*

| | | | |
|---|---|---|---|
| Emissions in natural environments | Shotgun cartridges to Natural soil<br>Litter (nature) to Natural soil<br>Fabric coatings to Natural soil (MP)<br>Shotgun cartridges to Surface water<br>Litter (nature) to Surface water | Location depends on the activities of the consumer and of hunters | Land use statistics: natural areas<br>Natural areas (from land use statistics) around the water bodies |
| Emissions through combined sewer overflows | CSO to Surface water<br>CSO (small) to Surface water<br>CSO (MP) to Surface water (MP) | Sewer Overflows | Sewer Overflows |
| Emissions through storm water | Storm water to Surface water<br>Storm water (MP) to Surface water (MP)<br>Industry water (MP) to Surface water (MP) | Storm water outlets | Sewer Overflows |
| Emissions through wastewater treatment plants | Secondary WWT (small) to Surface water<br>Secondary WWT (MP) to Surface water (MP)<br>Tertiary WWT (MP) to Surface water (MP) | WWTP effluent outlets | WWTP effluent outlets |

Emissions occurring from sewer overflows were regionalized using combined sewer overflows (CSO) locations and volumes discharged (Mutzner et al., 2016). The volume discharged is calculated from the published dataset by multiplying the wastewater influent to the WWTP and the time the CSOs were active.

The point emissions were attributed to the closest water body. The nearest water body to the point emission was identified using the *st_nearest_feature* and *st_distance* functions in the *sf* package in R.

### 2.9. Regionalization

For emissions to air and soil, the geodatasets were converted to rasters using the function *rasterFromXYZ* from the *raster* package in R, while making sure that the extent of the different rasters was identical. The traffic geodataset which consisted of vectors was then projected on a raster object with the same resolution and extent as the remaining geodatasets in QGIS. The native resolution of 100 m of the original rasters is kept for the calculation. The raster maps presented in this article are aggregated to a resolution of 1 km for visualization purposes. The final emission maps use the coordinate system EPSG 2056 (also called CH1903+ LV95). Vector data using the coordinate system CH1903 LV03 were converted by using the built-in functions in the *sf* and *rgdal* packages in R for vector data. The rasters based on the land use geodataset and the point sources to water (WWTP and sewer overflows) were converted by adding 2,000,000 m in the x direction and 1,000,000 m in the y direction. This manual coordinate transformation leads to minor deformations on the edges of Switzerland of up to 1.6 m (Federal Office of Topography swisstopo, 2016). This was preferred over a reprojection of the rasters in a new coordinate system where the data itself may undergo smoothing.

The emission flows are regionalized as follows:

$$\boldsymbol{f}_r = \frac{\boldsymbol{P}}{\sum_{i,j} \boldsymbol{P}_{ij}} \cdot f, \tag{1}$$

where $\boldsymbol{f}_r$ represents the regionalized emission flow, $\boldsymbol{P}$ the closest proxy available for the emission flow $f$. $\boldsymbol{f}_r$ and $\boldsymbol{P}$ can either be a matrix describing the individual cells of the raster or a vector describing the river segments or lake polygons. $\sum_{i,j} \boldsymbol{P}_{ij}$ represents the sum over all raster cells if the proxy is a raster or over all vector elements if the proxy is a vector. $f$ is the emission flow as calculated from the previous study, the full list of emission flows can be found in Table 1. All regionalized emission flows can then be summed to obtain the total emission maps of a specific polymer in soil, water or air, as macroplastic or MP:

$$\boldsymbol{f}_{\text{total}} = \sum_r \boldsymbol{f}_r. \tag{2}$$

All operations were performed in R using the *sf* and *raster* packages. The scripts are available online.

## 3. Results

### 3.1. Summed maps of the emissions

The final emissions maps are a linear combination of the proxy maps with varying weights depending on the emission flows (Fig. 1). Depending on the polymer, specific proxies dominate the final emission map, as for example the traffic proxy for macroplastic emissions to soil for all polymers except LDPE and PP for which the agriculture proxy is also essential. The MP emissions to soil are mostly influenced by industry (in particular PS and EPS), agriculture (LDPE, PP and PET) and new buildings (HDPE and PVC). Both MP and macroplastic emissions to water are to a large extent influenced by sewer overflows at around at least 80% of the weight. The population around water bodies accounts for most of the remaining emissions of macroplastic, the WWTPs for MP. The emissions to air depend on three proxies only: industry, population and new buildings, which are each very relevant for at least one polymer: LDPE is exclusively influenced by industry, EPS by new buildings and PET almost exclusively by the population proxy.

The example of PET macroplastic emissions to soil is considered in more detail to illustrate the regionalization process. Six different proxies contribute to it: traffic, forests and other natural environments, population, agriculture, industry and new buildings (Fig. 2). 81% of the emissions of PET macroplastic are regionalized using the traffic network as proxy because of littering along roads, which is reflected in the final result with the traffic network standing out the most. The emissions of PET related to this proxy can reach high levels, with up to 13 kg/ha/year (kg/ha/a) emitted. 9% of the emissions of PET macroplastic are regionalized using the forests and other natural environments mostly due to littering in natural environments, giving a low emission background of around at most 0.1 kg/ha/a in the Alps. The remaining proxies contribute to features which are less prominent.

Once the contributions of all proxies are added, one obtains maps of the modelled emissions per material, environmental compartment and size of plastic (Figs. 2–4 and S4–S8). Maps of the 5% and 95% quantiles of the emission probability distributions were as well generated and are available upon request. In most maps, a large fraction of the emissions takes place in the Swiss plateau, which is the region extending from

Lake Constance in the Northeast to Lake Geneva in the Southwest where most of the human activities are concentrated in Switzerland. The main valleys in the Alps are also easily recognizable in most maps.

The macroplastic emission maps (Fig. 3 for PS and LDPE, Fig. 2 for PET and Fig. S4 for all polymers) can be coarsely categorized into two types, the first one in which the traffic network is the most preeminent feature and the second one where the whole area of the Swiss plateau appears as the main feature. This is in accordance with the weights used where most polymers are largely defined by the traffic and agriculture proxies (Fig. 1). LDPE and PP are the two polymers for which agriculture plays an important role, and for which the Swiss plateau appears as a band of higher emissions. The local emission rates of LDPE are within 0–0.01–20 kg/ha/a (minimum-median-maximum) and the local emission rates of PP are within 0–0.02–36 kg/ha/a. The remaining

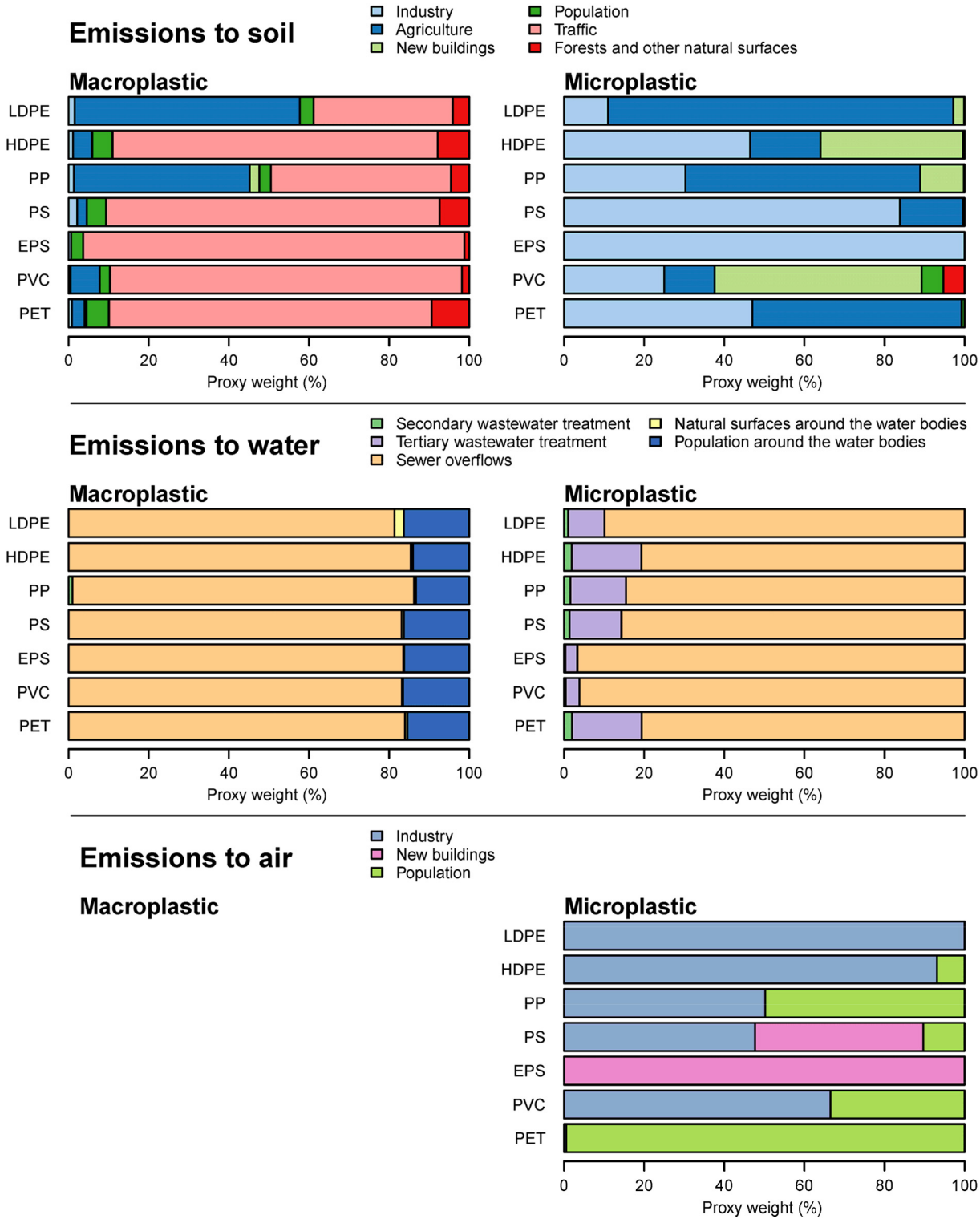


**Fig. 1.** Weight attributed to the different proxies for emissions to soil, water and air, as macroplastic and microplastic. The weights are calculated as proportions of the emission flows attributed to the respective proxies.

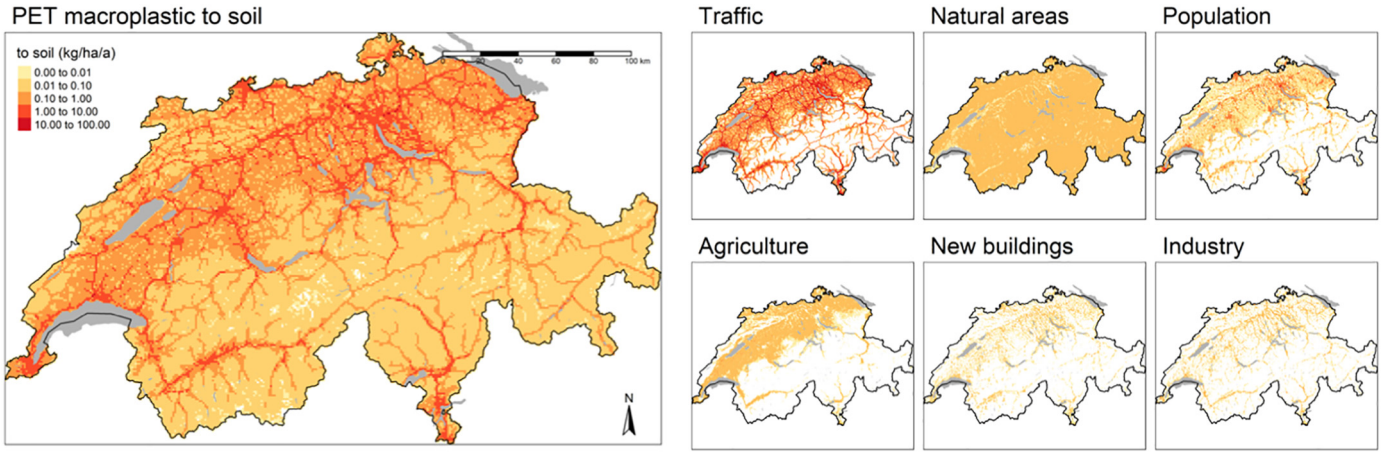


**Fig. 2.** Total emissions of PET macroplastic to soil (left) with the maps created from the six different proxies (right): traffic, forests and other natural areas, population, agriculture, new buildings and industry. The smaller maps are added to obtain the total map of PET macroplastic emissions.

polymers are mostly emitted along roadsides with emissions reaching a maximum for PET at 0–0.06–117 kg/ha/a. All of these polymers are used a lot in packaging and are littered along roadsides. In addition, accidental releases of construction material also cause large emissions to roadsides for PS (0–0.01–25 kg/ha/a), PVC (0–0.002–34 kg/ha/a) and EPS (0–0.001–11 kg/ha/a). The emission background visible in the mountainous regions is caused by the emissions in forests and natural soils. The largest emission flow associated to this proxy is littering in natural environments. PET, PP and HDPE present higher emission backgrounds in the Alps of at most 0.1 kg/ha/a emitted depending on the location. LDPE, PS, EPS and PVC display lower emission rates of at most 0.01 kg/ha/a.

Similarly, MP emission maps can be categorized into three types (Fig. 3 for LDPE and EPS and Fig. S5 for all polymers), the first one in which urban centres are central, the second one in which agriculture is more important and the third one in which the emission background over the Alps is larger. LDPE (0–0–2.6 kg/ha/a min-median-max), HDPE (0–0-13 kg/ha/a), PP (0–0-7.7 kg/ha/a) and PET (0–0-0.33 kg/ha/a) display a strong influence of the agriculture sector. On the other hand, PS (0–0-0.34 kg/ha/a), EPS (0–0-0.1 kg/ha/a) and PVC (0–0.001–22 kg/ha/a) are less influenced by the agriculture sector. Most of the MP emissions of all polymers are restricted to areas of high human activity, i.e. the Swiss plateau and the valleys. The higher emission background for PVC over the Alp region is caused by the wear of products outdoors producing MP.

The emissions of MP to air are restricted to areas with high human activity (Fig. 3 for PET and EPS and Fig. S8 for all polymers). The regionalization of the emissions to air depends exclusively on the proxies industry, population and new buildings (Fig. 1), which are all concentrated on the Swiss plateau and the valleys (Fig. S2). The urban centres are more accentuated for PET, PP and PVC. The industry and new building proxies are in regions of high human activity but further away from areas with high population densities. The largest local emission rates occur for PET in urban centres, and range within 0–0–22 kg/ha/a overall (min-median-max). PP follows similar emission rates at 0–0–11 kg/ha/a. The remaining polymers have lower emission rates: LDPE (0–0–0.08 kg/ha/a), HDPE (0–0–0.6 kg/ha/a), PS (0–0–3.8 kg/ha/a), EPS (0–0–1.6 kg/ha/a) and PVC (0–0–2.2 kg/ha/a).

Emission maps were also created for macroplastic and MP emissions to water (Fig. 4, S6, S7). PP macroplastic and PET MP emissions are shown in Fig. 4 with a zoomed map inset for each. Emissions to river segments are reported in kg/km/a and emissions to lakes in kg/ha/a. Most of the emissions are situated in areas with high human activity. The mean emission rate of macroplastic along river segments ranges between 0.062 kg/km/a for EPS and 1.5 kg/km/a for PET. For MP, this emission rate varies from 0.0025 kg/km/a for EPS to 0.11 kg/km/a for HDPE. In lakes, the average emission rates of macroplastic range from 0.0025 kg/ha/a for EPS to 0.061 kg/ha/a for PET. Similarly, between 0.0001 kg/ha/a of EPS and 0.004 kg/ha/a of HDPE are emitted as MP to lakes on average. The map insets presented in Fig. 4 show a more detailed view of the water bodies modelled. Sewer overflows have the largest weight for the final result for macroplastic consisting of any polymers at around 85% of the final result (Fig. 1) and the population around water bodies accounts for around 15%. Similarly, for MP, sewer overflows correspond to around 80–95% of the final result and the main remaining fraction is caused by emissions through tertiary wastewater treatment. Since the sewer overflow proxy has a similar weight for macroplastic and MP emissions of all polymers, the emission maps display similar tendencies within the river network and lakes. It is also clearly apparent from the map insets that there is no continuity of emission magnitudes along a river; each segment is independently calculated from the connected ones.

### 3.2. Correlation analysis

The population density has already been used as only proxy to regionalize emissions of plastic globally (Lebreton et al., 2017). It has never been investigated how well the population density can be used as a single proxy for plastic emissions. The correlation coefficient of the emissions to soil and air with the population density was calculated as a function of the plastic material and the raster resolution (Fig. 5). The rasters of emissions of microplastic to air, macroplastic and microplastic to soil were added for this analysis. The correlation coefficient increases with the cell size, reaching better correlation coefficients for a cell size of 10 km for most polymers. The best correlation is attained for HDPE, PS, EPS, PVC and PET at $r = 0.86–0.88$. A much worse correlation is found for PP at $r = 0.68$ and LDPE at $r = 0.56$. These two polymers are used extensively in agriculture and the regional distribution of agricultural activities does not coincide well with the population density. For cell sizes equal to or below 1 km, much lower correlation coefficients ($r < 0.5$) are obtained.

### 3.3. Influence of the input data

Large variations in local emission rates can be observed for the emission maps created using the mean, the 5th or 95th percentiles of the initial emission flow distributions (Fig. S9). The difference calculated as (95th percentile – 5th percentile)/mean is for all polymers in all raster cells in the case of macroplastic emitted to soil between 140% and 290%. The least variation is found for PP with a maximum of 234% and the highest for PVC with 293%. All of this variation is caused by the varying weights of the proxies in the three different scenarios. For LDPE, EPS

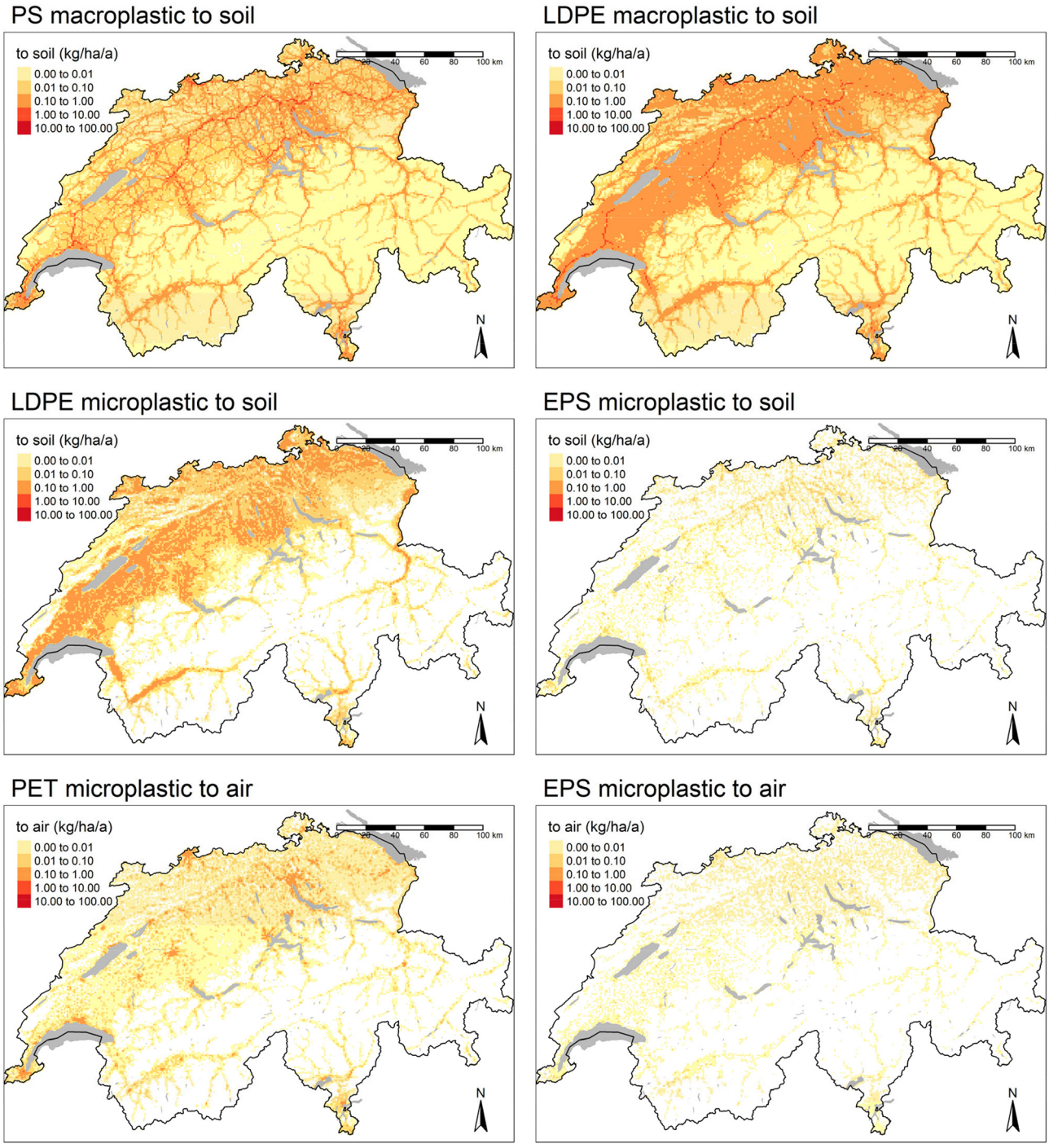


**Fig. 3.** Maps of the modelled emissions of PS and LDPE macroplastic to soil, of LDPE and EPS MP to soil and of PET and EPS MP to air. Equivalent maps for HDPE, PP, PS, EPS and PVC can be found in the SI in Figs. S4,S5 and S8.

and PVC, more variation is found on the Swiss plateau and in the alpine valleys. Less spatial variation is found for the remaining polymers, which are all influenced by littering in natural areas, on which a large uncertainty exists (Kawecki and Nowack, 2019).

Local emission rates can also be looked at from a density perspective (Fig. 6). In these density diagrams, the frequency of occurrence of the emission rates is shown on a logarithmic scale. The differences observed between the three scenarios are caused by the data used to model the emission flows (Kawecki and Nowack, 2019). The three spectra of emissions calculated with the mean and the quantiles have very similar shapes, with a few narrow peaks and smaller plateaus in the case of the emissions to soil and air. The spectra of emissions to rivers and lakes are much smoother in comparison, which is due to the fact that emissions to a single water body may originate from several point sources and a 500 m wide buffer used around the water body. Nevertheless, the three different spectra are separated by at least one order of magnitude for most environmental compartments, polymers and plastic sizes.

These density diagrams also reveal that there is no continuum in the emissions modelled for soil and air. This behaviour is mostly a consequence of the use of land-use statistics as proxies, since this geodataset contains categorical data. As a result, for a mean emission flow of 62 t for

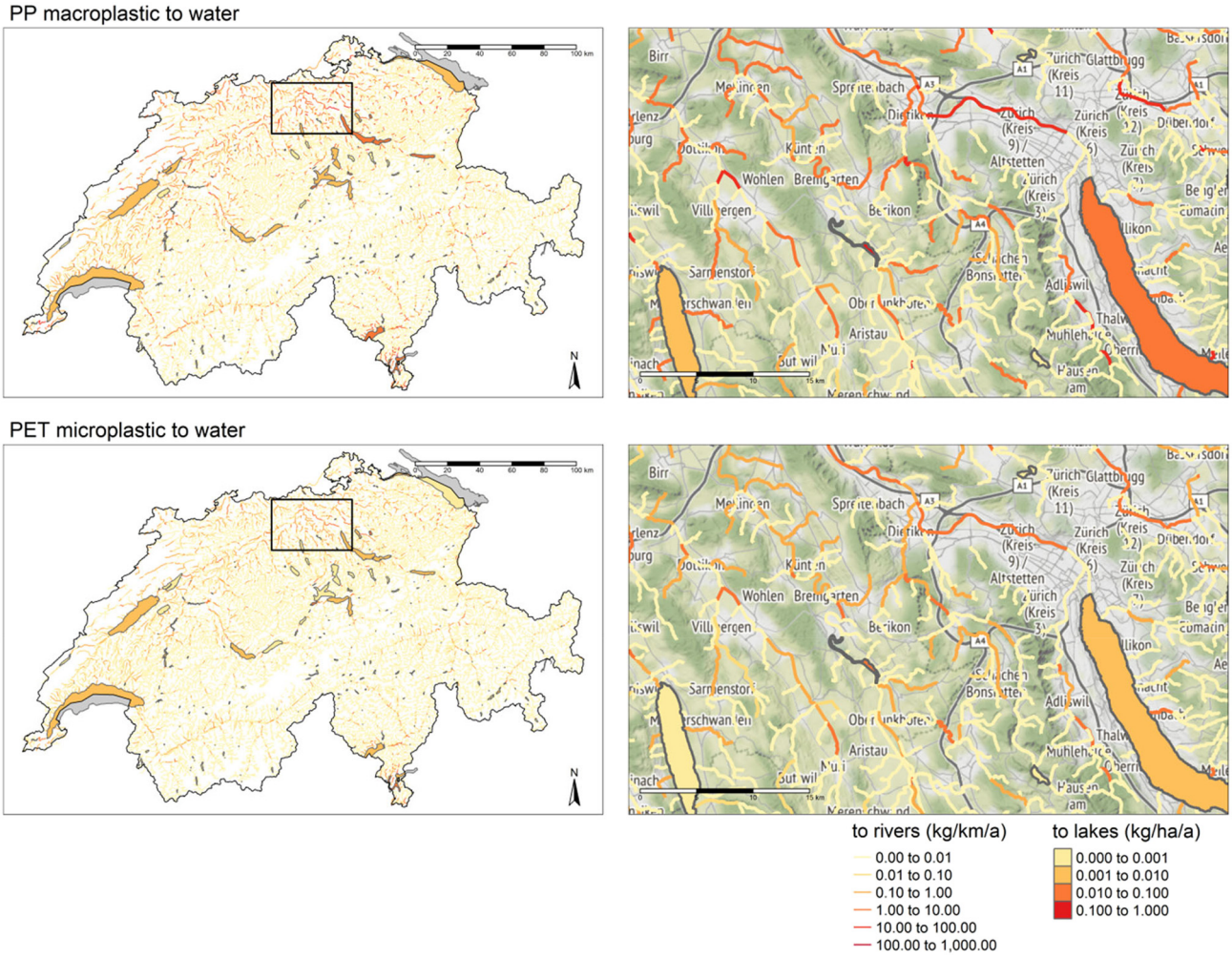


**Fig. 4.** Maps of the modelled emissions of PP macroplastic and PET microplastic to water. Emission maps for macroplastic and MP are presented in Figs. S6 and S7. The map insets on the right correspond to the area in the rectangles in the main maps. Map tiles by Stamen Design, under CC BY 3.0.
Data by OpenStreetMap, under ODbL.

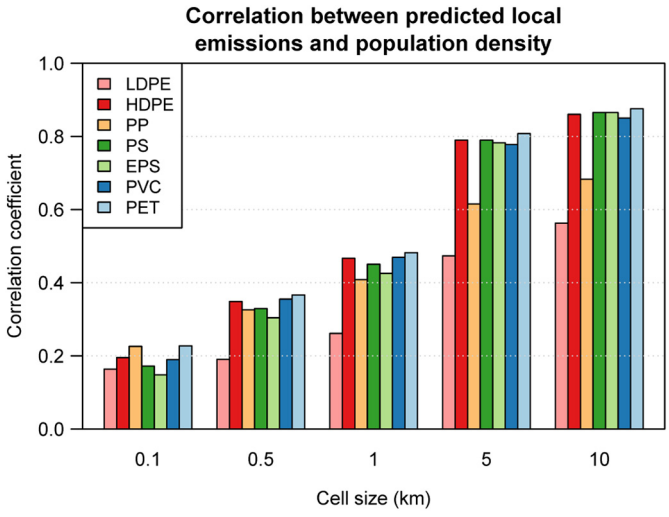


**Fig. 5.** Correlation coefficient of the raster of the emissions to soil and water with the population density raster. The correlation coefficients are grouped by raster resolution on the x-axis and the seven colours correspond to the seven polymers. (For interpretation of the references to colour in this figure legend, the reader is referred to the web version of this article.)

PP macroplastic regionalized using the agriculture proxy, and 458,038 cells where agriculture is present, one obtains an average emission of 62,000/458038 = 0.14 kg/ha/a, which corresponds to the largest peak in the red spectrum of the PP MP plot in Fig. 6. The smaller peak in the same graph situated around 1 kg/ha/a can be explained by new buildings and industry. Each of the 27,057 cells corresponding to new buildings obtained a local emission rate of 0.7 kg/ha/a, and each of the 41,006 cells corresponding to industry obtained a local emission rate of 0.78 kg/ha/a. The remaining features are caused by the population proxy, which is not a categorical dataset and thus doesn't create unique narrow peaks. Similarly, EPS MP emissions to soil also display a unique narrow peak of emissions, since only the industry proxy contributes to this emission. The spectrum for HDPE macroplastic emissions to soil is more intricate since 83% of the emissions are attributed to the traffic network which is not categorical. The two largest narrow peaks visible can be attributed to natural areas and agriculture. The PVC MP emissions to air depend only on the population proxy, which generates the first peak on the left and the plateau until $10^{-2}$, and on the industry proxy which generates the second peak at 0.15 kg/ha/a. The first peak caused by the population proxy can be attributed to the high number of cells with 3 inhabitants/ha which is the minimum in the geodataset for privacy purposes. A large number of cells or vector elements remain zero after the regionalization. The lowest share of cells with zero emissions is attained for macroplastic emissions to soil at 20%, since the littering to natural environments is spread out over the mountainous regions. For the

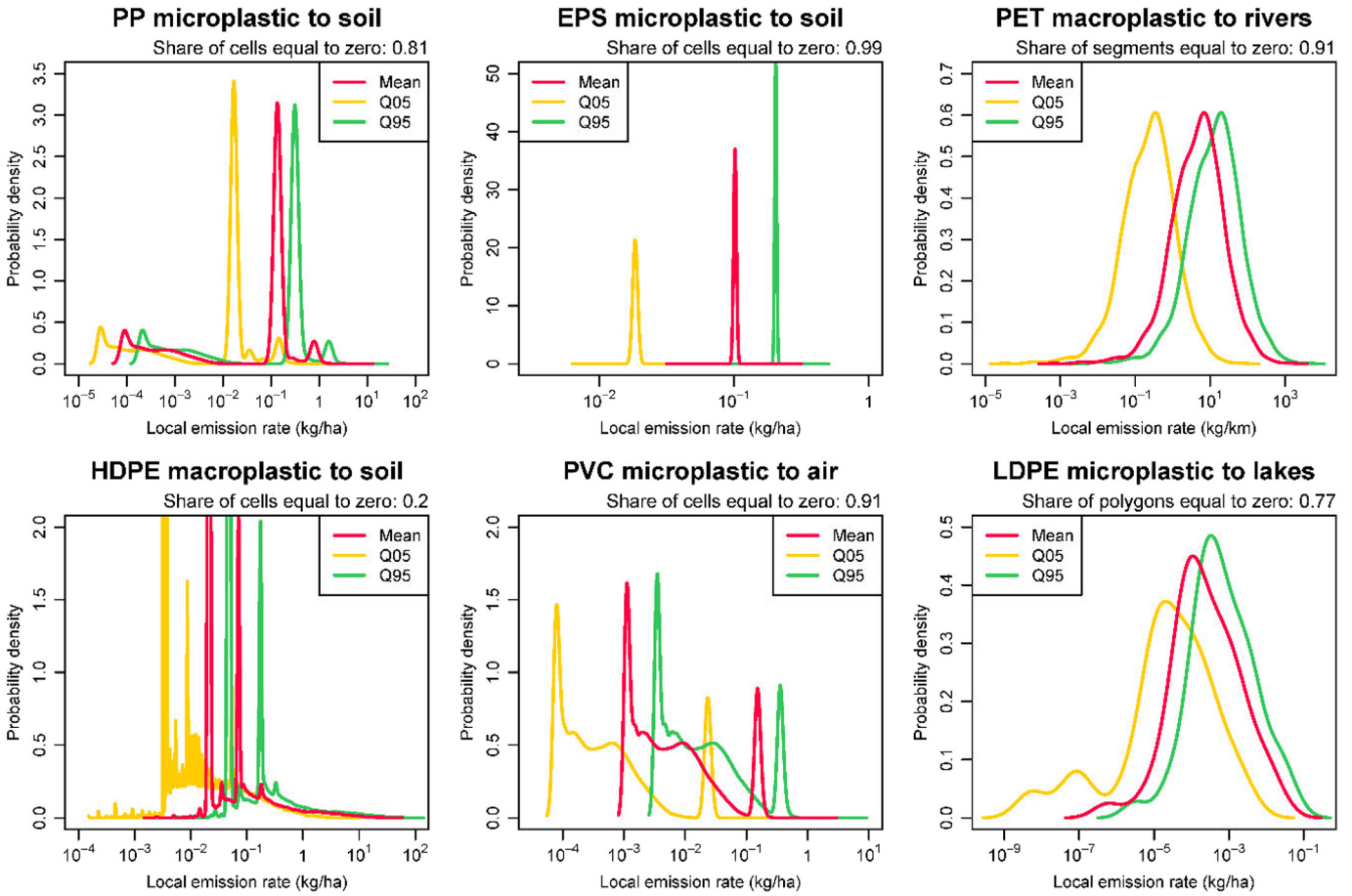


**Fig. 6.** Variability of the local emission rates of polymers to environmental compartments. The density functions are calculated using the *density* function from the *stats* package in R, after removal of the zero values. The fraction of cells or vector elements with zero values is shown below the title in each graph. The emission rates calculated using the mean of the emission flow distributions is shown in red, and the emission rates calculated using the quantiles are shown in yellow and green. (For interpretation of the references to colour in this figure legend, the reader is referred to the web version of this article.)

remaining emission maps, the share of elements with zero emissions varies from 20% to 91%.

## 4. Discussion

This study proposes a new approach to regionalize plastic emission flows in a specific region, by attributing emission flows to an appropriate geodataset used as proxy. A total of 35 maps were created using the mean emission flows, and a further 35 maps were created for the 5th and 95th percentiles each. These maps represent the modelled geographical repartition of previously modelled emission flows. These results reveal that the local emission rates can vary by at least two orders of magnitude depending on the polymer and receiving environmental compartment. The influence of the main applications of each polymer is as well visible, especially for polymers largely used in agriculture. The population density has already been used as only proxy to regionalize emission flows in previous studies (Lebreton et al., 2017). Our analysis shows that using the population density as only proxy could lead to large deviations in the spatial distribution of the plastic emissions at high resolution, in particular for polymers with major applications in agriculture as for example LDPE and PP. The positive correlation between the population density and our emission maps was to be expected, even more so at larger scales where less detail is visible. This also shows at what scale differences between the two modelling approaches can be noticed, which is important for all polymers for any resolution higher than 5 km, or for LDPE and PP already at 10 km. Although the included proxies may seem correlated in some areas, e.g. population and traffic density, this is not be the case in all areas, e.g. when considering the high traffic between cities. The regionalization of emission flows should therefore definitely consider more proxies than only the population density, especially for regions with large agricultural or industrial sectors. Deviations when using only population as proxy will still occur at a resolution of 10 km for all polymers but especially for LDPE and PP. For all lower resolutions, using the full suite of proxies is clearly advised in order to get reasonable predictions.

If emission maps on the scale of a city for example would be of particular interest, some adjustments in the proxies would be necessary. For example, considering a map of the human activity instead of the residence would add accuracy to the regionalization of littering and fibre emissions through wear in residential and natural areas. For natural areas, online databases for hiking trails and barbecue locations for example could be used to improve the precision of the proxy. The behaviour behind littering is known to be strongly dependent on the surroundings (Keizer et al., 2008). For a study of the amount littered at the scale of a city, other model types may be more appropriate as for example agent-based modelling (Rangoni and Jager, 2017) distinguishing the quality of the surroundings (Weaver, 2015).

It should be kept in mind that the present analysis is valid for Switzerland, and directly depends on the modelled life-cycle of the polymers used in Switzerland (Kawecki et al., 2018). Large variations in the uses of plastic in other countries might lead to a proxy having a much larger weight than the remaining proxies, for example in the case of agriculture (Scarascia-Mugnozza et al., 2012), and thus leading to a different geographical repartition of the plastic emissions. For

example, the agricultural sector can be more or less pronounced depending on the country, with varying plastic uses depending on the crops cultivated (Scarascia-Mugnozza et al., 2012). In a country with a strong agricultural sector, the validity of the population density as only proxy would be even lower. It should however be noted that the importance of traffic density and developed land use for plastic litter incidence was already demonstrated in a study in Iowa (Cowger et al., 2019), which argues in favour of the population density as single proxy. Further studies could shed some light on the validity of this assumption.

The model presented in this study relies on two types of data: the emission flow probability distributions and the map proxies. The uncertainty and validity of the model predicting the emission flows for Switzerland was already discussed in the original study (Kawecki and Nowack, 2019). In order to account for the uncertainty of the emission flows, maps using the 5th and 95th percentiles of the emission distributions were as well produced (Fig. S9).

Another type of uncertainty arises from the use of proxies to regionalize the emission flows. These proxies were chosen so that they should be representative of the behaviour underlying the emissions. In the density plots displayed in Fig. 6, narrow peaks in the local emission rates are observed, which are a consequence of the limited degree of detail in the categorical geodatasets. Since four out of the six raster proxies used for soil and air emissions rely on land-use statistics, emissions attributed to these proxies can only take a single value, which leads to a multitude of raster cells showing the same emissions. It is reasonable to assume that a certain variation occurs within such an emission type following variations in use intensity and use type as for example different crops in the case of agriculture, or varying levels of use of natural areas. Moreover, no differences between different parts of the country with respect to the emission flows are included. It should also be noted that only the emissions from Switzerland are included, which is important especially when considering the magnitude of the emissions to water bodies where a contribution from neighbouring countries takes place such as for Lake Constance (from Germany and Austria) and Lake Geneva (from France).

Validation is an important step in model development. While MP concentrations in freshwater are available from an array of studies, very few measurements of emission flows are available which could be used to validate the results of the here presented model. The comparison of our modelled emission data with published environmental concentration data would not make sense, since our model only includes emissions, without including environmental fate processes, and therefore cannot predict environmental concentrations. There is a prevalence of secondary microplastic in the environment, which is not predicted from our emission data without including fragmentation processes occurring in the environment. Moreover, there are not sufficient concentration data in soils available, and most of the novelty of our work is to provide maps for emissions to soil, and not only to water. The only Swiss-specific emission data that is available is from a study examining the MP release from 28 WWTPs based on a single measurement per WWTP effluent and visual identification of the MP (Cabernard et al., 2016). The MP release has been estimated using the MP concentration in the effluent and the average dry weather discharge rate. When comparing these estimates to our predictions, one finds that our predictions are a factor of 2.3 higher. A correlation coefficient of $r = 0.78$ was found between the two datasets, with a root mean squared error (RMSE) of 15 kg/a (compared to a minimum of 0.66 kg/a and maximum of 93 kg/a in our predictions) (see Fig. S10). Most of the error can be attributed to one single WWTP that treats around 45% of the water out of the 28 WWTPs considered for this comparison. If this datapoint is removed, the RMSE is reduced to 4.90 kg/a while the correlation coefficient drops to 0.41. Considering the multitude of uncertainty sources influencing both estimates, we consider the agreement between measured and predicted values is an indication that the implementation of the wastewater emission part of the model is capturing the actual emissions quite well.

The maps provided in this work represent emissions and should not be confused with concentration maps. The regionalization of emissions is a first step towards a fate model for macro- and microplastic. Based on the results of this study, a fate model could be adapted to account for all the processes occurring in the environment such as fragmentation, fluvial transport, runoff and sedimentation to name but a few (Besseling et al., 2017; Hoellein et al., 2019; Williams and Simmons, 1997). Since the fate of different plastics in freshwater environments depends on polymer density and product application (Schwarz et al., 2019), a distinction between different polymers is essential as provided in this work. Littering has been suggested as the main plastic source in several instances (Kawecki and Nowack, 2019; Kiessling et al., 2019), so the fragmentation of macroplastic to MP would need to be implemented. Such a fate model would then permit to predict environmental concentrations in soil and water of macroplastic and MP, which in turn could enable to perform regionalized risk assessments.

## CRediT authorship contribution statement

**Delphine Kawecki:** Conceptualization, Investigation, Software, Writing - original draft. **Bernd Nowack:** Conceptualization, Writing - review & editing, Supervision, Project administration.

## Declaration of competing interest

The authors declare that they have no known competing financial interests or personal relationships that could have appeared to influence the work reported in this paper.

## Acknowledgements

This work was supported by the Swiss Federal Office for the Environment (FOEN). The authors would like to thank Frédéric Guhl and Andreas Catillaz from FOEN, Olaf Koenig from the Swiss Federal Statistical Office, Edith Durisch-Kaiser from AWEL, Livia Cabernard from ETH Zürich and Lena Mutzner from Eawag for providing support or access to geographical datasets.

### *Model availability*

The R scripts written to perform the calculations are available at:
https://doi.org/10.5281/zenodo.3960301
The generated dataset is available here:
https://doi.org/10.5281/zenodo.3960287

## Appendix A. Supplementary data

Supplementary data to this article can be found online at https://doi.org/10.1016/j.scitotenv.2020.141137.

## References

Adam, V., Yang, T., Nowack, B., 2019. Toward an ecotoxicological risk assessment of microplastics: comparison of available hazard and exposure data in freshwaters. Environ. Toxicol. Chem. 38, 436–447. https://doi.org/10.1002/etc.4323.

Battulga, B., Kawahigashi, M., Oyuntsetseg, B., 2019. Distribution and composition of plastic debris along the river shore in the Selenga River basin in Mongolia. Environ. Sci. Pollut. Res., 14059–14072 https://doi.org/10.1007/s11356-019-04632-1.

Bauer-Civiello, A., Critchell, K., Hoogenboom, M., Hamann, M., 2019. Input of plastic debris in an urban tropical river system. Mar. Pollut. Bull. 144, 235–242. https://doi.org/10.1016/j.marpolbul.2019.04.070.

Besseling, E., Quik, J.T.K., Sun, M., Koelmans, A.A., 2017. Fate of nano- and microplastic in freshwater systems: a modeling study. Environ. Pollut. 220, 540–548. https://doi.org/10.1016/j.envpol.2016.10.001.

Browne, M.A., Galloway, T.S., Thompson, R.C., 2010. Spatial patterns of plastic debris along estuarine shorelines. Environ. Sci. Technol. 44, 3404–3409. https://doi.org/10.1021/es903784e.

Cabernard, L., Durisch-Kaiser, E., Vogel, J.-C., Rensch, D., Niederhauser, P., AWEL Gewässerschutz, 2016. Mikroplastik in Abwasser und Gewässern. Aqua Gas 7, 78–85.

Cascadia Consulting Group Inc, 2005. Washington 2004 State Litter Study: Litter Generation and Composition Report.
Castro-Jiménez, J., González-Fernández, D., Fornier, M., Schmidt, N., Sempéré, R., 2019. Macro-litter in surface waters from the Rhone River: plastic pollution and flows to the NW Mediterranean Sea. Mar. Pollut. Bull. 146, 60–66. https://doi.org/10.1016/j.marpolbul.2019.05.067.
Cowger, W., Gray, A.B., Schultz, R.C., 2019. Anthropogenic litter cleanups in Iowa riparian areas reveal the importance of near-stream and watershed scale land use. Environ. Pollut. https://doi.org/10.1016/j.envpol.2019.04.052.
de Souza Machado, A.A., Kloas, W., Zarfl, C., Hempel, S., Rillig, M.C., 2017. Microplastics as an emerging threat to terrestrial ecosystems. Glob. Chang. Biol. https://doi.org/10.1111/gcb.14020.
Dikareva, N., Simon, K.S., 2019. Microplastic pollution in streams spanning an urbanisation gradient. Environ. Pollut. 250, 292–299. https://doi.org/10.1016/j.envpol.2019.03.105.
Dris, R., Gasperi, J., Rocher, V., Saad, M., Renault, N., Tassin, B., 2015. Microplastic contamination in an urban area: a case study in greater Paris. Environ. Chem. 12, 592–599. https://doi.org/10.1071/EN14167.
Eerkes-Medrano, D., Thompson, R.C., Aldridge, D.C., 2015. Microplastics in freshwater systems: a review of the emerging threats, identification of knowledge gaps and prioritisation of research needs. Water Res. 75, 63–82. https://doi.org/10.1016/j.watres.2015.02.012.
Eriksen, M., Mason, S., Wilson, S., Box, C., Zellers, A., Edwards, W., Farley, H., Amato, S., 2013. Microplastic pollution in the surface waters of the Laurentian Great Lakes. Mar. Pollut. Bull. 77, 177–182. https://doi.org/10.1016/j.marpolbul.2013.10.007.
Essel, R., Engel, L., Carus, M., Ahrens, R.H., 2015. Sources of Microplastics Relevant to Marine Protection in Germany.
Federal Office for the Environment FOEN, 2011. VSA Kennzahlen. Obtained upon Req.
Federal Office for the Environment FOEN, 2015. Géodonnées sur la subdivision de la Suisse en bassins versant [WWW Document]. URL https://www.bafu.admin.ch/bafu/fr/home/themes/eaux/etat/cartes/geodonnees-sur-la-subdivision-de-la-suisse-en-bassins-versant.html.
Federal Office for the Environment FOEN, 2017. Adresses des stations d'épuration avec mention de leur capacité de traitement.
Federal Office of Topography swisstopo, 2016. Formulas and Constants for the Calculation of the Swiss Conformal Cylindrical Projection and for the Transformation between Coordinate Systems.
Fischer, E.K., Paglialonga, L., Czech, E., Tamminga, M., 2016. Microplastic pollution in lakes and Lake shoreline sediments - a case study on Lake Bolsena and Lake Chiusi (central Italy). Environ. Pollut. 213, 648–657. https://doi.org/10.1016/j.envpol.2016.03.012.
Gasperi, J., Dris, R., Bonin, T., Rocher, V., Tassin, B., 2014. Assessment of floating plastic debris in surface water along the Seine River. Environ. Pollut. 195, 163–166. https://doi.org/10.1016/j.envpol.2014.09.001.
Goldstein, M.C., Titmus, A.J., Ford, M., 2013. Scales of spatial heterogeneity of plastic marine debris in the Northeast Pacific Ocean. PLoS One 8. https://doi.org/10.1371/journal.pone.0080020.
Hartmann, N.B., Hüffer, T., Thompson, R.C., Hassellöv, M., Verschoor, A., Daugaard, A.E., Rist, S., Karlsson, T., Brennholt, N., Cole, M., Herrling, M.P., Hess, M.C., Ivleva, N.P., Lusher, A.L., Wagner, M., 2019. Are we speaking the same language? Recommendations for a definition and categorization framework for plastic debris. Environ. Sci. Technol. 53, 1039–1047. https://doi.org/10.1021/acs.est.8b05297.
Hoellein, T.J., Shogren, A.J., Tank, J.L., Risteca, P., Kelly, J.J., 2019. Microplastic deposition velocity in streams follows patterns for naturally occurring allochthonous particles. Sci. Rep. 9, 1–11. https://doi.org/10.1038/s41598-019-40126-3.
Horton, A.A., Walton, A., Spurgeon, D.J., Lahive, E., Svendsen, C., 2017. Microplastics in freshwater and terrestrial environments: evaluating the current understanding to identify the knowledge gaps and future research priorities. Sci. Total Environ. 586, 127–141. https://doi.org/10.1016/j.scitotenv.2017.01.190.
Kawecki, D., Nowack, B., 2019. Polymer-specific modeling of the environmental emissions of seven commodity plastics as macro- and microplastics. Environ. Sci. Technol. 53, 9664–9676. https://doi.org/10.1021/acs.est.9b02900.
Kawecki, D., Scheeder, P., Nowack, B., 2018. Probabilistic material flow analysis of seven commodity plastics in Europe. Environ. Sci. Technol. 52, 9874–9888. https://doi.org/10.1021/acs.est.8b01513.
Keizer, K., Lindenberg, S., Steg, L., 2008. The spreading of disorder. Science (80-. ). 322, 1681–1685. https://doi.org/10.1126/science.1161405.
Kiessling, T., Knickmeier, K., Kruse, K., Brennecke, D., Nauendorf, A., Thiel, M., 2019. Plastic pirates sample litter at rivers in Germany – Riverside litter and litter sources estimated by schoolchildren. Environ. Pollut. 245, 545–557. https://doi.org/10.1016/j.envpol.2018.11.025.
Koelmans, A.A., Mohamed Nor, N.H., Hermsen, E., Kooi, M., Mintenig, S.M., De France, J., 2019. Microplastics in freshwaters and drinking water: critical review and assessment of data quality. Water Res. 155, 410–422. https://doi.org/10.1016/j.watres.2019.02.054.
Lebreton, L.C.M., Zwet, J. Van Der, Damsteeg, J., Slat, B., Andrady, A., Reisser, J., 2017. River plastic emissions to the world's oceans. Nat. Commun. 8, 1–10. https://doi.org/10.1038/ncomms15611.
Mani, T., Hauk, A., Walter, U., Burkhardt-Holm, P., 2016. Microplastics profile along the Rhine River. Sci. Rep. 5, 17988. https://doi.org/10.1038/srep17988.
Morritt, D., Stefanoudis, P.V., Pearce, D., Crimmen, O.A., Clark, P.F., 2014. Plastic in the Thames: a river runs through it. Mar. Pollut. Bull. 78, 196–200. https://doi.org/10.1016/j.marpolbul.2013.10.035.
Mutzner, L., Staufer, P., Ort, C., 2016. Model-based screening for critical wet-weather discharges related to micropollutants from urban areas. Water Res. 104, 547–557. https://doi.org/10.1016/j.watres.2016.08.003.
Nizzetto, L., Futter, M., Langaas, S., 2016. Are agricultural soils dumps for microplastics of urban origin? Environ. Sci. Technol. 50, 10777–10779. https://doi.org/10.1021/acs.est.6b04140.
OpenStreetMap Foundation, 2019. OpenStreetMap [WWW Document]. CC BY-SA. URL https://www.openstreetmap.org/copyright.
Rangoni, R., Jager, W., 2017. Social dynamics of littering and adaptive cleaning strategies explored using agent-based modelling. J. Artif. Soc. Soc. Simul. 20.
Rech, S., Macaya-Caquilpan, V., Pantoja, J.F., Rivadeneira, M.M., Jofre Madariaga, D., Thiel, M., 2014. Rivers as a source of marine litter - a study from the SE Pacific. Mar. Pollut. Bull. 82, 66–75. https://doi.org/10.1016/j.marpolbul.2014.03.019.
Rios Mendoza, L.M., Balcer, M., 2018. Microplastics in freshwater environments: a review of quantification assessment. TrAC - Trends Anal. Chem 113, 402–408. https://doi.org/10.1016/j.trac.2018.10.020.
Ryberg, M.W., Hauschild, M.Z., Wang, F., Averous-Monnery, S., Laurent, A., 2019. Global environmental losses of plastics across their value chains. Resour. Conserv. Recycl. 151, 104459. https://doi.org/10.1016/j.resconrec.2019.104459.
Scarascia-Mugnozza, G., Sica, C., Russo, G., 2012. Plastic materials in European agriculture: actual use and perspectives. J. Agric. Eng. 42, 15–28. https://doi.org/10.4081/jae.2011.3.15.
Scheurer, M., Bigalke, M., 2018. Microplastics in Swiss floodplain soils. Environ. Sci. Technol. 52, 3591–3598. https://doi.org/10.1021/acs.est.7b06003.
Schultz, P.W., Bator, R.J., Large, L.B., Bruni, C.M., Tabanico, J.J., Brown Large, L., Bruni, C.M., Tabanico, J.J., 2013. Littering in context. Environ. Behav. 45, 35–59. https://doi.org/10.1177/0013916511412179.
Schwarz, A.E., Ligthart, T.N., Boukris, E., van Harmelen, T., 2019. Sources, transport, and accumulation of different types of plastic litter in aquatic environments: a review study. Mar. Pollut. Bull. 143, 92–100. https://doi.org/10.1016/j.marpolbul.2019.04.029.
Senozon AG im Auftrag des Bundesamts für Umwelt BAFU, 2017. sonBASE – Verkehrsdaten Schweiz 2015.
Sieber, R., Kawecki, D., Nowack, B., 2019. Dynamic probabilistic material flow analysis of rubber release from tires into the environment. Environ. Pollut. 113573. https://doi.org/10.1016/j.envpol.2019.113573.
Swiss Federal Statistical Office, (2013). Statistique de la superficie selon nomenclature 2004 – Standard [WWW Document]. Géodonnées la Stat. fédérale. URL https://www.bfs.admin.ch/bfs/fr/home/services/geostat/geodonnees-statistique-federale/sol-utilisation-couverture/statistique-suisse-superficie.html.
Swiss Federal Statistical Office, (2017). Statistique des bâtiments et des logements (StatBL) [WWW Document]. Géodonnées la Stat. fédérale. URL https://www.bfs.admin.ch/bfs/fr/home/services/geostat/geodonnees-statistique-federale/batiments-logements-menages-personnes/batiments-logements-des-2010.html.
Swiss Federal Statistical Office, (2018). Statistique de la population et des ménages (STATPOP) dès 2010 [WWW Document]. Géodonnées la Stat. fédérale. URL https://www.bfs.admin.ch/bfs/fr/home/services/geostat/geodonnees-statistique-federale/batiments-logements-menages-personnes/population-menages-depuis-2010.html.
Unice, K.M., Weeber, M.P., Abramson, M.M., Reid, R.C.D., van Gils, J.A.G., Markus, A.A., Vethaak, A.D., Panko, J.M., 2019. Characterizing export of land-based microplastics to the estuary - part I: application of integrated geospatial microplastic transport models to assess tire and road wear particles in the seine watershed. Sci. Total Environ. 646, 1639–1649. https://doi.org/10.1016/j.scitotenv.2018.07.368.
Wagner, S., Klöckner, P., Stier, B., Römer, M., Seiwert, B., Reemtsma, T., Schmidt, C., 2019. Relationship between discharge and river plastic concentrations in a rural and an urban catchment. Environ. Sci. Technol. 53, 10082–10091. https://doi.org/10.1021/acs.est.9b03048.
Weaver, R., 2015. Littering in context(s): using a quasi-natural experiment to explore geographic influences on antisocial behavior. Appl. Geogr. 57, 142–153. https://doi.org/10.1016/j.apgeog.2015.01.001.
Williams, A.T., Simmons, S.L., 1997. Movement patterns of riverine litter. Water Air Soil Pollut. 98, 119–139. https://doi.org/10.1007/BF02128653.
Zimmermann, L., Dierkes, G., Ternes, T.A., Völker, C., Wagner, M., 2019. Benchmarking the in vitro toxicity and chemical composition of plastic consumer products. Environ. Sci. Technol. 53, 11467–11477. https://doi.org/10.1021/acs.est.9b02293.
Zubris, K.A.V., Richards, B.K., 2005. Synthetic fibers as an indicator of land application of sludge. Environ. Pollut. 138, 201–211. https://doi.org/10.1016/j.envpol.2005.04.013.